Viktor BELDJAJEV, Indrek ROASTO

Tallinn University of Technology

Efficiency and Voltage Characteristics of the Bi-Directional Current Doubler Rectifier

Abstract. *This paper presents a detailed analysis of the bi-directional current doubler rectifier (CDR) that is a candidate topology for use in power electronic transformer (PET). Among various advantages the proposed current doubler rectifier offers a bi-directional power flow capability that is the major requirement for the PET. This paper provides the steady state analysis of the CDR in bi-directional operation. Input voltage boost properties of converters are compared for an ideal case. Finally, the impact of losses in the components on the voltage characteristics and efficiency are analysed.*

Streszczenie. *W artykule przedstawiono szczegółową analizę podwajającego prostownika dwukierunkowego (CDR), którego topologia może być użyta do konstrukcji transformatorów energoelektronicznych (PET). Wśród wielu zalet proponowany układ oferuje dwukierunkową możliwości przepływu energii, która jest głównym wymogiem dla PET. Niniejszy dokument przedstawia analizę stanu ustalonego CDR w działaniu dwukierunkowym. Właściwości zwiększania napięcia wejściowego tych przekształtników są porównywane dla przypadku idealnego. W części końcowej przeanalizowano wpływ strat w elementach na charakterystykę napięciową oraz sprawność układu (**Sprawność i charakterystyki napięciowe podwajającego prostownika dwukierunkowego).***

Keywords: bi-directional current doubler rectifier, steady state analysis, loss analysis, efficiency.
Słowa kluczowe: prostownik dwukierunkowy podwajający prąd, analiza stanu ustalonego, analiza strat, sprawność.

Introduction

Switching mode power supplies have been widely used in modern industry products to supply a stable DC voltage. In consideration of cost and efficiency, the conventional hard switching techniques are giving way to more economical topologies where zero voltage switching or zero current switching can be utilized. Typically, the flyback and forward converters are selected for low power applications, and a half bridge converter is used for medium power applications. Half- bridge topology has low cost in comparison to full bridge, however the full-bridge offers better performance in medium and high power applications [1].

Among different soft switching techniques, a full bridge (FB) converter with phase shift was proposed to improve the performance of hard switching converters. The aim of such technique is to achieve soft switching merely by use of only the leakage inductance and output capacitances of the controllable switches. However, the parasitic ringing generated by the large transformer leakage and external inductances and transformers stray capacitance can cause additional EMI problems [2]. One of such topologies, with the full-bridge on the primary side and current doubler rectifier on the secondary side was described in [1], where the ZVS conditions are analysed in a detail. Thorough coverage of the operation of such topology in the forward mode is presented in [3] - [6], where a detailed analysis can be found. However, using CDR in reverse mode has been proposed only by few authors [1], [7] - [9], thus a more detailed analysis is required.

In the current case the main application field is the DC/DC converter of a power electronic transformer (PET). In such application one of the main requirements is the bi-directional power flow capability [10] - [14]. The control task is to keep the voltages on both sides at a constant level. When selecting an appropriate topology it must be kept in mind that different boost factors may become a hindrance to achieving desired functionality. When designing the converter it is also important to take into account that losses in the components reduce the voltage boost and thus converter needs to have sufficient bandwidth to compensate losses. The proposed DC/DC FB converter with the current doubler rectifier (CDR) has a wide voltage regulation capability in a wide duty cycle range. Moreover, it is capable of utilizing the parasitic elements to achieve zero voltage switching.

This paper gives a detailed steady state analysis of the bi-directional CDR considering losses in the elements.

Circuit Configuration

The circuit topology of the proposed DC/DC converter is shown in Fig.1. The circuit consists of the controllable full bridge with 4 switches $T_1 \ldots T_4$ with their corresponding anti-parallel diodes $D_1 \ldots D_4$ and parasitic capacitances, a high frequency transformer TR and a CDR. In order to realize energy flow in two directions the diodes in traditional CDR are replaced with controllable switched T_6 and T_8 and traditional inductors are replaced with auxiliary transformers T_{aux1} and T_{aux2}. Additional auxiliary circuit is added to provide the freewheeling path for the leakage energy of the transformers, in case the duty cycle is lower than 50 % [1]. Auxiliary circuit redirects leakage energy of the transformers back to the low voltage side through the diodes thus preventing dangerous overvoltage to the switches. In addition, the transformers have higher inductance L than inductors used in the traditional CDR. The high frequency isolation transformer provides required voltage gain as well as the galvanic isolation between the input and output sides of the converter.

Two distinct operating modes of the converter are the forward and the reverse operating modes. In forward operating mode the energy is transferred from high voltage FB side to the low voltage side (buck mode). In reverse operating mode the energy is transferred from the low voltage CDR side to the high voltage side (boost mode).

The typical current and voltage waveforms of the converter in forward operating continuous conduction mode are shown in Fig.2. The FB is controlled with phase shifted PWM, with duty cycles near D_A = 0.5, whereas the phase shift determines the effective duty cycle of the converter. Phase shift provides the zero voltage switching capability and desired voltage gain. At the same time, only the diodes and auxiliary transformer primaries conduct on the CDR side. A capacitor is used to smoothen the output voltage.

The typical current and voltage waveforms in reverse operating continuous conduction mode are shown in Fig.3.

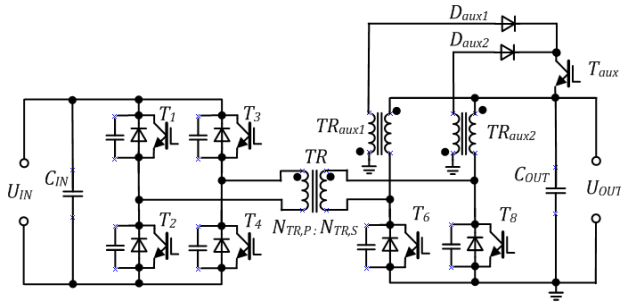

Fig.1. Main circuit of bi-directional current doubler rectifier

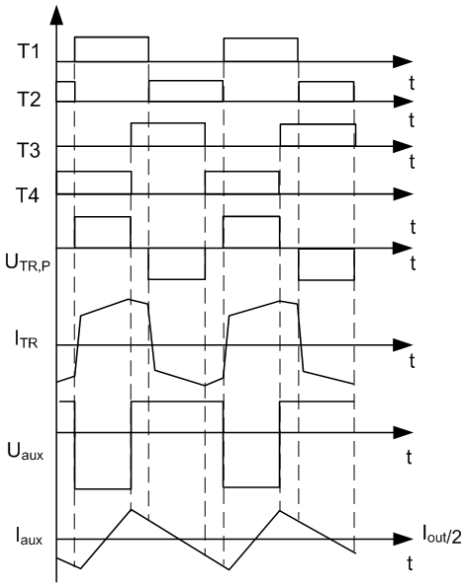

Fig.2. Typical waveforms for CDR in forward operating mode

Switches T_6 and T_8 on the CDR side are controlled with PWM, whereas the duty cycle of the switch can vary from 0…1. If the duty cycle is D_A > 0.5 then auxiliary path is disconnected. The power is transferred to the output during the turn ON of one switch. Energy stored in the auxiliary transformer is redirected into the HF transformer during the overlap of the control signals. At the same time only the diodes conduct on the FB side.

Main benefits of the proposed bi-directional CDR are zero voltage switching capability for the primary switches T_1...T_4 in a wide load range, achievable to utilize the energy stored in the output filter inductances. Moreover, CDR allows bi-directional energy flow control. Using a HF transformer reduces the size of the converter. Reduced current ripples due to the transformers and offer better thermal performance due to the current doubling effect. In addition the CDR has reduced transient response [1].

Steady State Analysis of the CDR

In the steady state analysis both the forward and the reverse operating modes are handled separately due their different control principles. To simplify the analysis, it is assumed that the auxiliary transformers TR_{aux1} and TR_{aux2}, as well as all transistors T_1…T_8 are identical (the same collector-emitter and freewheeling diode voltage drops). For the analysis, the skin and proximity effects in transformers are neglected.

The operating period T of one switch in the continuous conduction mode consists of active state t_A and zero state t_Z:

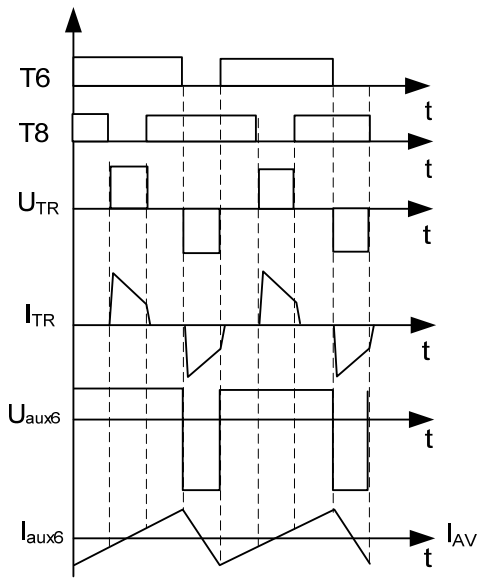

Fig.3. Typical waveforms for CDR in reverse operating mode

(1) $$T = t_A + t_Z$$

Equation (1) can also be represented with duty cycles

(2) $$\frac{t_A}{T} + \frac{t_Z}{T} = D_A + D_Z = 1,$$

where D_A and D_Z are the duty cycles of an active and zero states of a switch, correspondingly.

In the forward mode the effective duty cycle must be used. The effective duty cycle D_E for the CDR in forward mode depends on the phase shift value and can roughly be expressed by

(3) $$D_E = D_A - \varphi\,,$$

where φ is the phase shift value in p.u. between the two legs of FB.

The steady state analysis of both topologies is based on the fact that an average voltage over the auxiliary transformers during one operating period is zero:

(4) $$U_{TRaux} = \frac{1}{T}\int_{t}^{t+T} u_{TRaux}\,dt = 0\,,$$

In the forward operating mode, the current in the auxiliary transformer is half of the output current, whereas the output current is determined by the ratio of the output voltage and the load resistance. Each diode in the CDR conducts each half cycle. The four basic equivalent circuits for forward operating mode are shown in Fig.4. More detailed analysis can be found in [2], [5]. During the effective duty cycle the voltage over the auxiliary transformer TR_{aux1} is equal to the difference between the HF transformer's secondary and output voltages (see Fig.4, a). During this period the transformer secondary voltage is equal to multiplication of the input side voltage and transformer turns ratio.

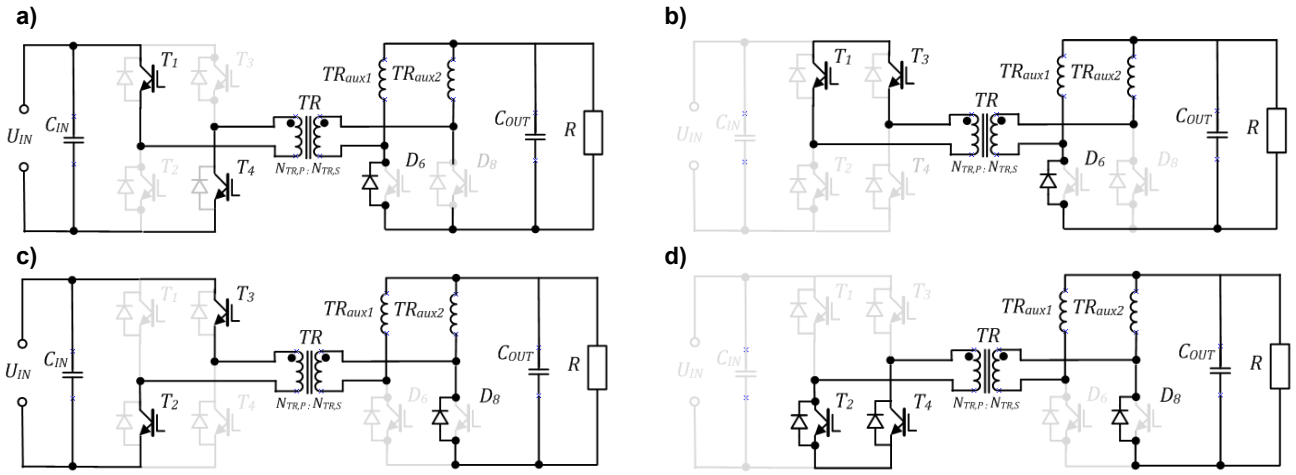

Fig. 4. Switching states of CDR in forward mode. a) active state of T_1, T_4; b) overlap of T_1, T_3; c) active state of T_2, T_3; d) overlap of T_2, T_4

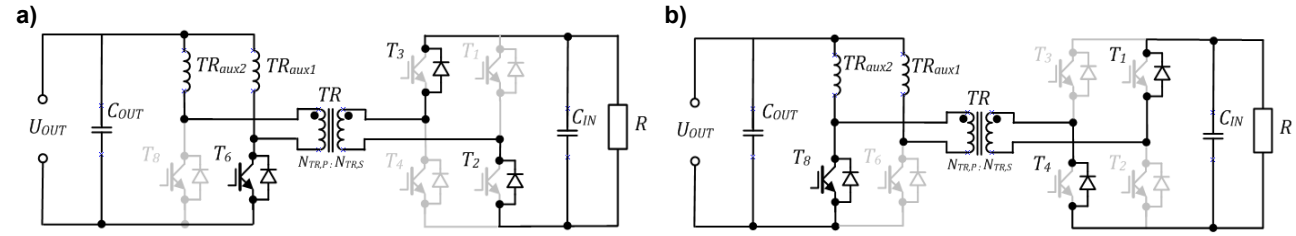

Fig. 5. Switching states of CDR in reverse mode. a) active state of T_6; b) zero state of T_6.

During the overlap of the transistors T_1 and T_3 (see Fig.4, b) the voltage over the TR_{aux1} is equal to the output voltage. Next half switching cycle is similar to previous one, and voltage over the auxiliary transformer TR_{aux1} is equal to the output voltage. During the rest of the period the voltage over the auxiliary transformer is equal to the output voltage. Thus according to the requirement (4) we get

$$(5) \qquad \left(U_{IN} \cdot N_{TR} - U_{OUT}\right) \cdot D_E + U_{OUT} \cdot (1 - D_E) = 0$$

where N_{TR} is the transformers turns ratio, U_{IN} is the voltage on the input side and U_{OUT} voltage on the output side of the converter. From here the output voltage can be evaluated as follows

$$(6) \qquad U_{OUT} = U_{IN} \cdot N_{TR} \cdot D_E$$

In the reverse operating mode the output side voltage acts now like a source and the input side voltage must be estimated. Voltage over the auxiliary transformer is equal to the output side voltage during the active state of the switch T_6, as shown in Fig.5, a. During the overlap of the control signals for T_6 and T_8 the voltage over the auxiliary transformer TR_{aux1} remains the same as can be seen in Fig.3. During the zero state of switch T_6 the voltage over the auxiliary transformer TR_{aux1} is equal to the difference between output side voltage and HF transformer voltage. Equation for the voltage over the auxiliary transformer with $D_A > 0.5$, considering also requirement (4), can be written in a following way

$$(7) \qquad U_{OUT} \cdot D_A + \left(U_{OUT} - \frac{U_{IN}}{N_{TR}}\right) \cdot D_Z = 0\,,$$

from where the input side voltage can be derived:

$$(8) \qquad U_{IN} = \frac{U_{OUT} \cdot \left(D_A + D_Z\right)}{D_Z} \cdot N_{TR} = \frac{U_{OUT} \cdot N_{TR}}{1 - D_A}$$

Impact of Component Losses

In the previous section the lossless models of the CDR were presented. However in practise the voltage boost properties of CDR can be seriously affected by the losses in the components. Moreover, the DC/DC stage of PET comprises the biggest part of overall losses [14]. In the DC/DC stage the following losses are present: conduction losses of the passive and active components, switching losses and core losses. Conduction losses are caused by active resistances in the wires, transformer windings and switches (collector-to-emitter voltage drop, reverse recovery diode voltage drop). Switching losses comprise the turn-on, turn-off and diode reverse recovery losses. The core losses occur in the HF and auxiliary transformers. Previous steady-state analysis included only the analysis of conduction losses.

The conduction losses are more critical on the low voltage and higher current side, where voltage drops over the elements affect the efficiency significantly. For more careful estimation of the operating characteristics of the converter the loss elements, such as winding resistances in the transformers and voltage drops in semiconductors, should be added to the model. In the following analysis the winding losses in auxiliary transformers are represented by the resistance r_{aux}, winding resistance on transformer primary r_{TR_P} and on transformer secondary r_{TR_S}, voltage drop in diodes during the conduction state is U_D. In addition, IGBTs with saturation voltage U_{CE} were used.

As the converter is intended to be used in the isolation stage of power electronic transformer, it is necessary for the converter to keep specified voltage levels on both sides. The specified voltage levels for input and output sides are as follows

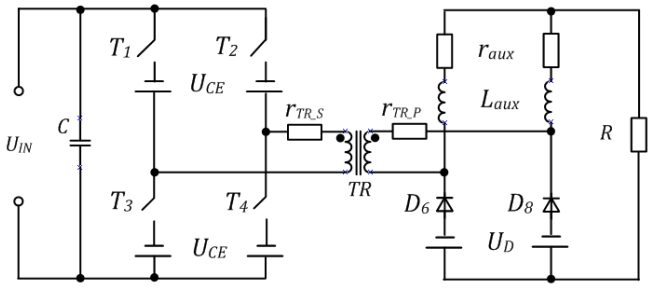

Fig. 6. Equivalent circuit of the lossy model of the CDR. a) forward mode; b) reverse mode

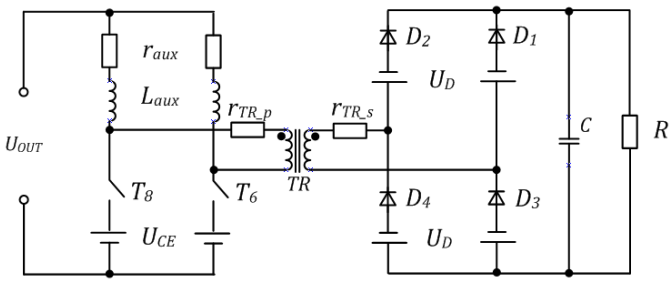

Fig. 7. Equivalent circuit of the lossy model of the CDR. a) forward mode; b) reverse mode

U_{IN} = 200 V; U_{OUT} = 30 V

In the case of reverse operating mode the output side is handled as an input. In further examples the duty cycles for each operating mode are selected so that desired voltage level could be achieved. It must be noticed that the losses can significantly reduce the voltage gain of the converter, thus the required duty cycle must always be bigger than the one obtained with (6) or (8).

Forward Operating Mode

The equivalent circuit considering the losses in components for forward operating mode is shown in Fig.6. On FB side the losses occur due to collector-to-emitter voltage drops U_{CE} of transistors $T_1 \ldots T_4$. On the CDR side the diode voltage drop U_D occurs in diodes D_6, D_8. All transformers have also voltage drop due to winding resistances. The equation (5) can now be extended with adding the losses in the components. And thus we get equation (9), where R designates the load resistance. Output voltage can be thus evaluated according to (10). The current in auxiliary transformer is half the output current.

In order to demonstrate the impact of losses in the components on the voltage characteristics in forward operating mode, then investigated topology is compared mathematically with following parameters:

U_{IN} = 200 V; U_{CE} = 1.8 V; U_D = 1.6 V;
R = 10 Ω; r = 1 mΩ; D_E = 0.45; N_{TR} = 1/3;

where r designates the winding resistance values for auxiliary transformers, and HF transformer resistances on both sides. The corresponding dependency is shown in Fig.8, a. It can be seen that losses become more significant with the increase of the power (duty cycle) and decrease the voltage boost in comparison to the ideal case.

Reverse operating mode

In the reverse operating mode the energy is transferred from the low voltage output side to the high voltage input side. The equivalent circuit considering the losses in the components is shown in Fig.7. In this case, the collector-to-emitter voltage drop U_{CE} occurs in the transistors T_6, T_8 on CDR side and voltage drop U_D occurs in the diodes $D_1 \ldots D_4$ on FB side. As the converter operates with the duty cycle $D_A > 0.5$ then the auxiliary path is disabled and thus not shown in the drawing.

$$(9)\quad U_{aux} = -\left[\left(U_{IN} - 2U_{CE} - I_{aux}N_{TR}r_{TR\_P}\right)\cdot N_{TR} - U_{OUT} - U_D - I_{aux}(r_{aux} + r_{TR\_S})\right]\cdot D_E + \left(U_{OUT} + U_D + I_{aux}r_{aux}\right)\cdot\left(1 - D_E\right) = 0$$

$$(10)\quad U_{OUT} = -\frac{2R\cdot(U_D + 2N_{TR}U_{CE}D_E - N_{TR}U_{IN}D_E)}{D_E\cdot\left(r_{TR\_P}N_{TR}^2 + r_{TR\_S}\right) + 2R + r_{aux}}$$

$$(11)\quad \begin{cases} U_{aux} = \left(U_{OUT} - U_{CE} - \dfrac{U_{IN} - 2U_D + I_{TR\_P}\cdot r_{TR\_P}}{N_{TR}} - I_{aux}\cdot(r_{aux} + r_{TR\_S})\right)\cdot(1 - D_A) + \left(U_{OUT} - U_{CE} - I_{aux}r_{aux}\right)\cdot D_A = 0 \\ I_C = \left(\dfrac{I_{aux}}{N_{TR}} - I_{IN}\right)\cdot 2(1 - D_A) - I_{IN}\cdot\left(2D_A - 1\right) = 0 \end{cases}$$

$$(12)\quad U_{IN} = -\frac{2R(D_A - 1)\cdot(2D_AU_D - 2U_D - N_{TR}\cdot U_{CE} + N_{TR}U_{OUT}}{2R + r_{TR\_P} + N_{TR}^2\left[r_{TR\_S}\cdot(1 + D) + r_{aux})\right] - D\left[2R\cdot(2 + D) + r_{TR\_P}\right]}$$

$$(13)\quad I_{aux} = \frac{N_{TR}\left[2U_D\left(D - 1\right) - N_{TR}\left(U_{CE} - U_{OUT}\right)\right]}{2R + r_{TR\_P} + N_{TR}^2\left[r_{TR\_S}\cdot(1 + D) + r_{aux})\right] - D\left[2R\cdot(2 + D) + r_{TR\_P}\right]}$$

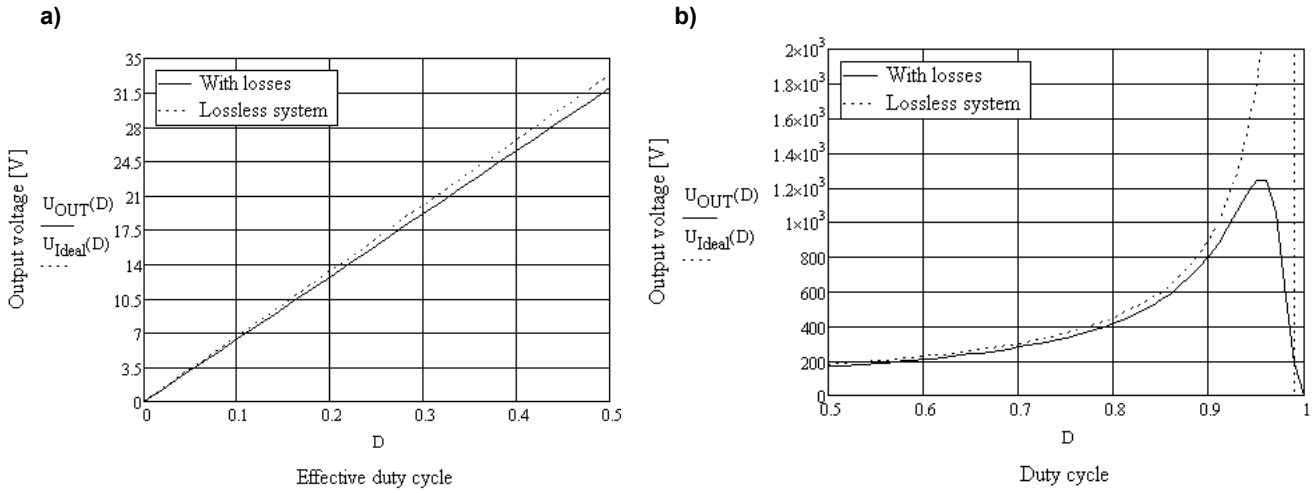

Fig. 8. Comparison of idealized and practical output characteristics of the CDR. a) forward mode; b) reverse mode.

The equation (7) can now be extended to adding the losses of all elements. In order to solve the equation, the current in auxiliary transformer is also needed to be estimated. This can be achieved from the capacitor current, which average is equal to zero over the whole switching period. Eq (11) presents the corresponding equation system. Solving this equation system gives us the solution for the input side voltage which can be estimated according to (12). The current in auxiliary transformer can be obtained with (13). Current on the output side is thus twice the auxiliary current.

In order to demonstrate the impact of losses in the reverse operating mode, then investigated topology is compared mathematically with the following parameters:

U_{IN} = 200 V; U_{CE} = 1,8 V; U_D = 1,6 V;

R = 100 Ω; r = 1 mΩ; D_E = 0.55; N_{TR} = 3;

The corresponding dependency is shown in Fig.8, b. It can be seen that without losses the voltage boost can be infinitely high. However, in the high duty cycle region losses become very significant and thus reduce the voltage boost rapidly to zero.

Efficiency estimation

In the following section the efficiency is estimated using the mathematical model and experimental results. The models were verified on the 1 kW experimental prototype. The 6 IGBTs with switching frequency of 40 kHz are used. The parameters of the experimental prototype are presented in Table 1 and a picture of the prototype is shown in Fig.9. The voltage and current waveforms on the input and output side in forward mode are shown in Fig.10. Same characteristics for reverse mode are shown in Fig.11. It can be seen that specified voltage levels are effectively achieved on both sides of the converter.

The overall efficiency of the CDR can be estimated using the ratio of the output power P_{OUT} and the input power P_{IN},

$$\eta = \frac{P_{OUT}}{P_{IN}} = \frac{U_{OUT}^{\ 2}}{R \cdot U_{IN} \cdot I_{IN}} \cdot 100\% \tag{14}$$

By inserting the equations (10), (12), (13) into (14), the efficiency of the converter in both operating modes was calculated. The results are presented in the Table 2. In forward mode the efficiency 86.7% was achieved while in the reverse mode this number is only 72.6 %. This difference can be explained with higher conduction losses in the CDR due to higher currents during reverse mode. The difference between mathematical and experimental results can be explained with the fact, that mathematical model did not take switching and core losses of the transformers into account.

Table 1. The parameters of the experimental prototype

Parameter	Value
Input side voltage (U_{IN})	200 V
Output side voltage (U_{OUT})	30 V
Switching frequency (f_s)	40 kHz
HF transformer turns ratio (N_{TR})	3
Inductance of HF transformer (L_μ)	1 mH
Inductance of auxiliary transformer ($L_{\mu aux}$)	248 μH
Transformer winding resistances	10 mΩ
IGBT (IRG7Ph42ud1pbf) saturation voltage (U_{CE})	1,8 V
Freewheeling diode voltage drop (U_D)	1,6 V
Duty cycle (D)	0.43 (forw) / 0.56 (rev)
IGBT driver type	IR4427 Dual low side driver IR2181 High side driver

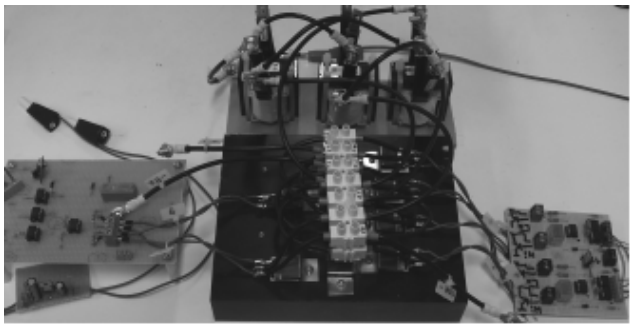
Fig. 9. Experimental prototype of CDR

High voltage peaks were observed in the input and output voltages, as shown in Figs.10 and 11. Those peaks, typical to current doubler rectifier, are caused by the auxiliary transformers T_{aux1}, T_{aux2}. The problem could be solved by implementing proper snubbers.

Table 2. The efficiency of the CDR in defined operating point

Operating mode	Forward	Reverse
Estimated	86.7 %	72.6 %
Experimental	80.7 %	64 %

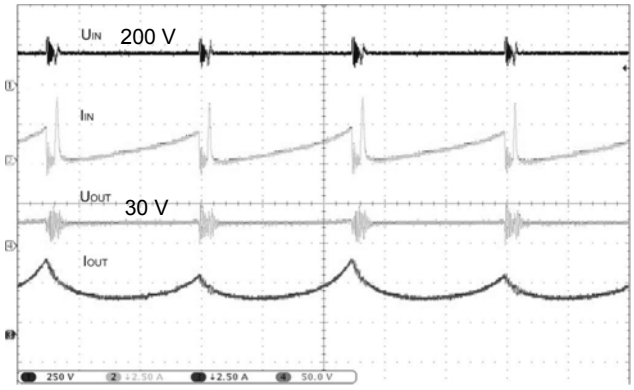

Fig. 10. Input and output side voltage and current waveforms in forward mode

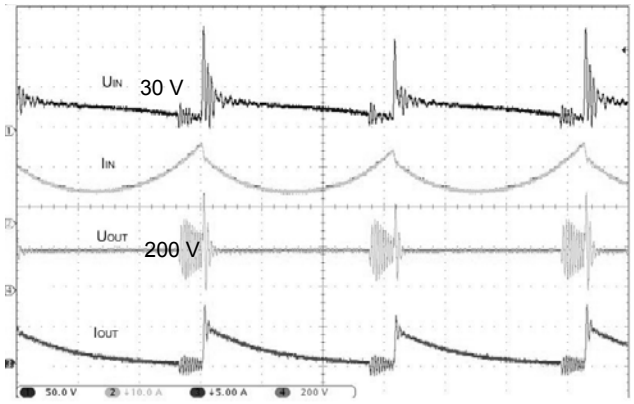

Fig. 11. Input and output side voltage and current waveforms in reverse mode

Conclusion

The paper presented a detailed analysis of the voltage characteristics of the CDR in forward and reverse operating modes. Special attention was paid on the voltage characteristics and efficiency of the investigated topology. Bi-directional CDR as a candidate topology for a DC/DC stage of the power electronic transformer (PET) is the most critical part of the system considering the overall efficiency. In the steady state analysis mathematical models with and without losses were derived and analysed. It was found that for the same operating parameters the converter can operate at the maximum efficiency of 87 % in forward mode and with 72.6 % in reverse mode. The results were verified on the experimental prototype, where the measured efficiencies are 80.7 % and 64 % correspondingly. Voltage characteristics were studied and quite high voltage peaks were observed in the input and output voltage.

In general, relatively low efficiency and high voltage peaks could hinder use of such converter in PET. Future work will include further investigation of CDR to improve its voltage characteristics and efficiency, with proper selection of components and by adding snubber circuits.

Acknowledgement

This research was supported by Estonian Ministry of Education and Research (Project SF0140016s11), Estonian Science Foundation (Grant ETF8687) and European Social Fund´s project Doctoral School of Energy and Geotechnology II.

REFERENCES

[1] Lin, B.-R; Huang, K; Wang, D.; , " Analysis and implementaton of full bridge converter with current doubler rectifier," Proc. IEE Electric Power Appl., vol. 152, no. 5, pp. 1193-1202, 2005.

[2] Chiu, H.J.; Lin, L.W.; Su, Y.C.;Mou, S,C.; , " A phase shfted zero voltage transition full bridge converter with current doubler synchrnous rectification," SICE 2004 Annual Conference, vol. 1, pp. 60-65, 2004.

[3] Beldjajev, V.; Roasto, I.; Vinnikov, D.; , "Analysis of current doubler rectifier based high frequency isolation stage for intelligent transformer," Compatibility and Power Electronics (CPE), 2011 7th International Conference-Workshop , vol., no., pp.336-341, 1-3 June 2011

[4] Kutkut, N.H.; Luckjiff, G.; "Current mode control of a full bridge DC-DC converter with a two inductor rectifier" PESC '97 Page(s): 203 -209 vol.1

[5] Kutkut, N.H.; "A full bridge soft switched telecom power supply with a current doubler rectifier" INTELEC 97., 19-23 Oct 1997 Page(s):344 -351

[6] Kutkut, N.H.; Divan, D.M.; Gascoigne, R.W.; "An improved full bridge zero-voltage switching PWM DC-DC converter using a two inductor rectifier "Industry Applications Society Annual Meeting, 1993., Conference Record of the1993 IEEE,2-8 Oct1993,Page(s):1065- 1072vol.2

[7] Flores, L.A.; Garcia, O.; Oliver, J.A.; Cobos, J.A. "High Frequency Bi-Directional DC/DC Converter Using Two Inductor Rectifier". IECON 2006, pp. 2793 – 2798.

[8] Liang, Y.; Lehman, B. Isolated Two-Inductor Boost Converter with One Magnetic Core. APEC '03. IEEE, pp. 879 – 885.

[9] Yungtaek, Y.; Jovanovic, M. M. New Two-Inductor Boost Converter with Auxiliary Transformer. Power Electronics, IEEE Transactions on vol. 19, Issue 1, Jan. 2004, pp. 169 – 175.

[10] van der Merwe, J.W.; du T. Mouton, H.; , "The solid-state transformer concept: A new era in power distribution," AFRICON, 2009. AFRICON '09. , vol., no., pp.1-6, 23-25 Sept. 2009.

[11] Heinemann, L.; Mauthe, G.; , "The universal power electronics based distribution transformer, an unified approach," Power Electronics Specialists Conference, 2001. PESC. 2001 IEEE 32nd Annual , vol.2, no., pp.504-509 vol.2, 2001.

[12] Falcones, S.; Xiaolin Mao; Ayyanar, R.; , "Topology comparison for Solid State Transformer implementation," Power and Energy Society General Meeting, 2010 IEEE , vol., no., pp.1-8, 25-29 July 2010.

[13] Hengsi Qin; Kimball, J.W.; , "A comparative efficiency study of silicon-based solid state transformers," Energy Conversion Congress and Exposition (ECCE), 2010 IEEE , vol., no., pp.1458-1463, 12-16 Sept. 2010.

[14] Beldjajev, V.; Roasto, I.; Lehtla T.; , "Intelligent Transformer: Possibilities and Challenges" RTU, 2011. , pp . 14 Okt 2011.

***Authors**: M. Sc, Dipl. Ing. Viktor Beldjajev, Tallinn University of Technology, Dep. of Electrical Drives and Power Electronics, Ehitajate Tee 5, Tallinn Estonia. E-mail: vbeldjajev@gmail.com; PhD, Dipl. Ing. Indrek Roasto, Tallinn University of Technology, Dep. of Electrical Drives and Power Electronics, Ehitajate Tee 5, Tallinn Estonia. E-mail: indrek.roasto@ieee.org*